Received: 18 January 2021 | Revised: 18 March 2021 | Accepted: 25 March 2021

DOI: 10.1002/ardp.202100029

FULL PAPER

ARCH PHARM DPhG
Archiv der Pharmazie

Synthesis and biological evaluation of new coumarin derivatives as cytotoxic agents

Fatma A. Ragab[1] | Amal A. M. Eissa[1] | Samar H. Fahim[1] | Mohammad A. Salem[2,3] | Mona A. Gamal[1] | Yassin M. Nissan[1,2]

[1]Pharmaceutical Chemistry Department, Faculty of Pharmacy, Cairo University, Cairo, Egypt

[2]Pharmaceutical Chemistry Department, Faculty of Pharmacy, October University for Modern Sciences and Arts (MSA), Giza, Egypt

[3]School of Life and Medical Sciences, University of Hertfordshire hosted by Global Academic Foundation, Cairo, Egypt

Correspondence
Samar H. Fahim, Pharmaceutical Chemistry Department, Faculty of Pharmacy, Cairo University, El-Kasr El-Eini St, Cairo 11562, Egypt.
Email: samarhfmy@hotmail.com

Abstract

New coumarin derivatives **9a–f**, **10a–e**, and **11a–f** were synthesized and evaluated for their cytotoxic activity against a human breast cancer cell line (MCF-7). All compounds exhibited good activity in the nanomolar range, using doxorubicin and erlotinib as positive controls. The most active compound **9d** with IC_{50} of 21 nM was tested against the HCT-116, HepG-2, A549, and SGC-7901 cell lines, with IC_{50} values of 0.021, 0.170, 0.028, and 0.11 μM, respectively. Compound **9d** was further investigated for its ability to suppress the expression of epidermal growth factor receptor (EGFR). Compound **9d** decreased the concentration of EGFR by 87%, using erlotinib as a positive control. A docking study revealed similar or higher scores than for erlotinib and similar binding poses providing interactions with the hinge region of the tyrosine kinase (TK). Besides the effect on expression, this in silico investigation predicts the possibility of direct binding between the new coumarin derivatives and the EGFR TK. Moreover, computational calculation for ADME properties for the most active compounds **9d**, **9e**, **10c**, and **11c** revealed the expected high gastrointestinal tract absorption, moderate water solubility with no central nervous system toxicity, and druglikeness.

KEYWORDS
anticancer activity, coumarin, EGFR, MCF-7, pyrazoline

1 | INTRODUCTION

Cancer has been one of the most challenging cell disorders for decades. The mortality rate is ranked on the second position among all diseases.[1] Despite the continuous discovery of new strategies and molecules for treatment, emerging resistance and dangerous side effects are still the main barriers for radical cure.[2] Exploration of new molecules based on scaffolds of natural compounds can contribute in reducing such harmful side effects.[3] Among these scaffolds, coumarins[4,5] have exhibited a wide range of biological activity. These various activities were studied by medicinal chemists' synthetic schemes and biological evaluations. Antibacterial,[6,7] anticoagulant,[8–10] antioxidant,[11,12] anti-inflammatory,[13,14] and anticancer activities[15–18] have been exhibited by coumarin derivatives. Several mechanisms of action have explained the cytotoxic activity for such derivatives. These mechanisms varied between apoptosis induction,[19] cell cycle arrest,[20] inhibition of telomerase,[21] and inhibition of tyrosine kinases (TKs).[22] Among these TKs, some coumarin derivatives have exhibited a potent inhibitory effect toward epidermal growth factor receptor (EGFR). Daphentin (**I**), a 7,8-dihydroxycoumarin derivative, has been identified as an EGFR inhibitor[23] (Figure 1). A series of 3-carboxamide derivatives (**II**) was synthesized and evaluated as EGFR suppressors.[24] Furthermore, the substitution of the coumarin scaffold at position 3 has been reported in several investigations of new anticancer coumarin derivatives with enhanced activity.[25] Position 8 of the coumarin ring was studied by Amin et al. by substituting with pyrazoline moieties leading to good activity of the synthesized

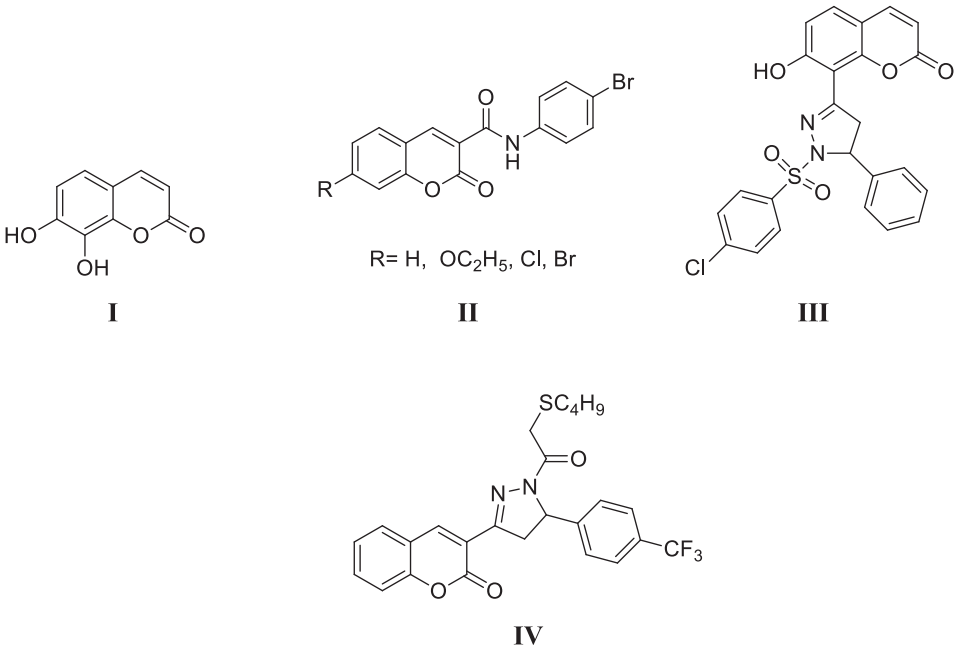

FIGURE 1 Coumarin derivatives with a potent anticancer activity

derivatives. They have reported that compound **III** (Figure 1) exhibited good activity toward PI3K enzyme.[26] In addition to this hybrid of coumarin–pyrazoline that was reported, several such hybrids were studied between these two moieties. Among these hybrids, one was introduced by Wu et al. The researchers in this investigation have synthesized a coumarin–pyrazoline hybrid with good activity toward several cancer cell lines. Compound **IV** (Figure 1) has exhibited potent activity toward telomerase enzyme with IC_{50} of 0.92 μM.[21] However, several reports examined the cytotoxic activity of synthesized coumarin derivatives against a variety of cell lines. Coumarin hybrids were tested against BT20 human breast carcinoma, SK-Mel 128 melanoma, DU-145 prostate carcinoma, and A549 lung carcinoma with IC_{50} range of 3.1–36.7 μg/ml.[27] Other coumarin–pyrazole hybrids were tested against MCF-7 cell line with IC_{50} range of 7.9–31.2 μg/ml.[28] Many coumarin derivatives had also been tested against other cell lines with IC_{50} range of 30.7–500 μg/ml.[29] However, other coumarin–triazole hybrids were tested against many cancer cell lines with IC_{50} range of 0.26–50 μg/ml.[30]

On the basis of these findings and as a continuation for our synthetic schemes[31–37] to explore the anticancer activity of new small organic compounds, this current investigation describes the synthesis and biological evaluation of new coumarin hybrids as cytotoxic agents. This investigation aimed to find new potent candidates based on the natural scaffold (coumarin).

2 | RESULTS AND DISCUSSION

2.1 | Chemistry

The synthetic routes for the preparation of the target hybrids are outlined in Schemes 1–4. Two key coumarin precursors, 8-acetyl-7-hydroxy-4-methylcoumarin **4** and 3-acetylcoumarin **6**, were required. Precursor **4** was synthesized according to Pechmann reaction by reacting resorcinol **1** and ethyl acetoacetate in the presence of acid catalyst to give 7-hydroxy-4-methylcoumarin **2**, which upon acetylation and Fries rearrangement gave 8-acetyl-7-hydroxy-4-methylcoumarin **4**[38–40] (Scheme 1).

However, precursor **6** was obtained via Knoevenagel condensation of salicylaldehyde **5** and ethyl acetoacetate in the presence of piperidine[41] (Scheme 2).

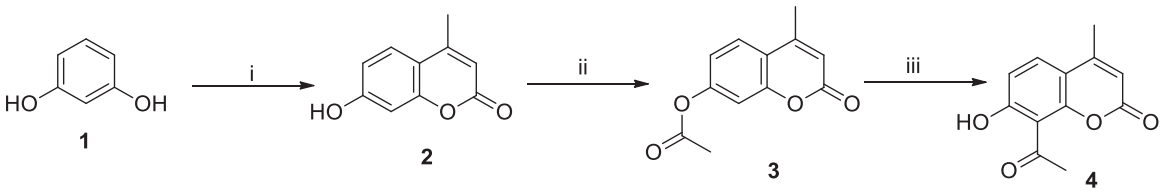

SCHEME 1 Synthesis of compound **4**. Reagents and conditions: (i) Ethyl acetoacetate, conc. H_2SO_4, room temperature overnight; (ii) acetic anhydride, reflux, 1.5 h; (iii) $AlCl_3$, heat 170°C, 2 h

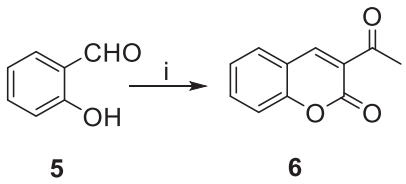

SCHEME 2 Synthesis of compound **6**. Reagents and conditions: (i) Ethyl acetoacetate, piperidine, room temperature, 20 min

Acetyl derivatives **4** and **6** were converted to the corresponding chalcones **7a–f** and **8a–f**, respectively, via Claisen–Schmidt condensation with various aromatic aldehydes in the presence of piperidine and acetic acid[42,43] (Scheme 3). These chalcones have been utilized to synthesize different N^1-substituted pyrazolines. The new coumarin–pyrazoline hybrids containing thiourea skeleton, **9a–f**, have been synthesized by reaction of **7a–f** with thiosemicarbazide under acidic condition (Scheme 3). ^{1}H nuclear magnetic resonance (NMR) of **9a–f** revealed two doublets of doublets at 2.88–3.24 and 3.58–4.02 ppm, assigned to the two protons on the diastereotopic center C4, and a third doublet of doublet at 5.30–5.88 ppm, assigned to the C5-H_X. There are three coupling constants: $J_{a\text{-}b}$ = 16.3–18.5 Hz, $J_{a\text{-}x}$ *cis* 2.8–3.2 Hz, $J_{b\text{-}x}$ *trans* 11.4–12.2 Hz. In addition, singlet peaks were observed at 6.22–6.90 ppm, assigned to C3 proton of chromene, two doublet peaks at 6.99–7.43 and at 7.72–7.82 ppm, assigned to C5 and C6 protons, respectively. The protons of the phenyl substituents were observed at the expected chemical shifts and integral values. In addition, two exchangeable signals at 7.99–8.64 and 10.84–11.04 ppm attributed to NH_2 and OH protons, respectively, appeared. ^{13}C NMR of **9e** exhibited signals at 31.86 and 76.14 ppm, assigned to C4 and C5 of pyrazoline, respectively, and at 180.07 ppm for (C=S), the aromatic carbons appeared at the expected region.

The 1-(4-chlorophenyl)pyrazoline derivatives **10a–e** were obtained in high yields through the reaction of the appropriate chalcones **8a–e** with 4-chlorophenylhydrazine hydrochloride ethanol in the presence of acetic acid (Scheme 4). ^{1}H NMR spectra of the obtained derivatives exhibited three doublet of doublet signals at δ = 3.21–3.23, 3.96–4.01, and 5.49–5.58 ppm, corresponding to the three protons of pyrazoline CH_2 and CH due to vicinal and geminal coupling showing a prominent ABX system ($J_{Ha\text{-}Hx}$ = 5.1–5.96 Hz, $J_{Hx\text{-}Hb}$ = 12.2–12.4 Hz and $J_{Ha\text{-}Hb}$ = 17.96–18.04 Hz). In addition, chalcones **8a–f** were cyclized to the corresponding 4,5-dihydro-1*H*-pyrazol-1-yl)benzenesulfonamide derivatives **11a–f** by refluxing the appropriate chalcones with 4-hydrazinylbenzenesulfonamide hydrochloride in ethanol in the presence of acetic acid (Scheme 4). ^{1}H NMR spectra exhibited three doublet of doublet signals at δ = 3.27–3.30, 4.00–4.05, and 5.62–5.82 ppm, corresponding to the three protons of pyrazoline CH_2 and CH, again showing a prominent ABX system. Also, an exchangeable peak resonated at 7.06–7.07 ppm, corresponding to the NH_2 protons.

2.2 | Biological evaluation

2.2.1 | Antiproliferative activity

Seventeen new derivatives were tested for their in vitro cytotoxic activity against MCF-7 breast cancer cell line. The most active derivatives were further tested against four different cell lines (HCT-116 colon cancer cell line, HepG-2 hepatic cancer cell line, A549 lung cancer cell line, and SGC-7901 gastric cancer cell line) using the 3-(4,5-dimethylthiazol-2-yl)-2,5-diphenyl tetrazolium bromide (MTT) assay.[44,45] Doxorubicin and erlotinib were used as a positive control. The activity was expressed by median growth inhibitory concentration (IC_{50}), and it is presented in Tables 1 and 2. The results revealed that, against MCF-7, 8 compounds out of the 17 tested compounds were more potent than doxorubicin with IC_{50} values in the range of 0.021–8.300 μM (IC_{50} of doxorubicin: 0.800 μM). However, compared with erlotinib, an EGFR inhibitor, 16 compounds

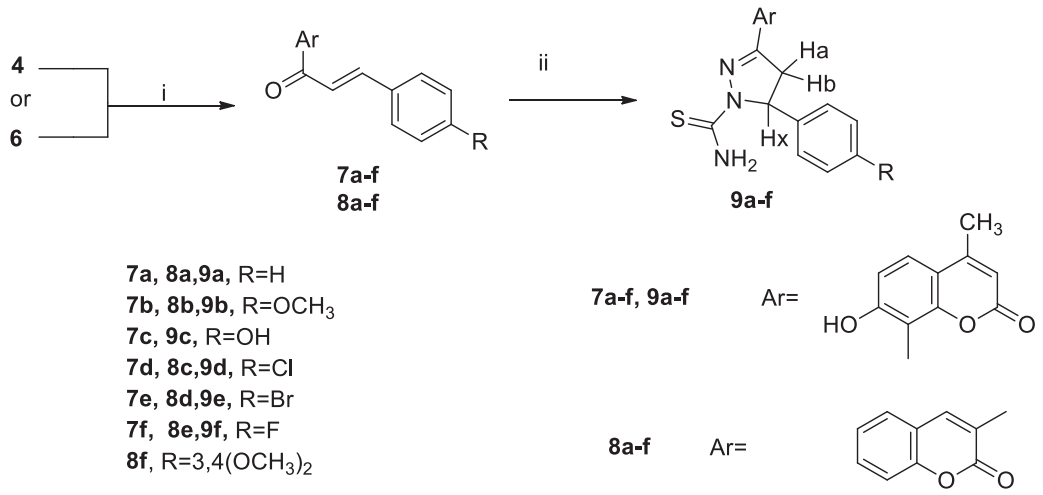

SCHEME 3 Synthesis of the target compounds **9a–f**. Reagents and conditions: (i) Ar-CHO, glacial acetic acid–piperidine/ethanol, reflux, 4 h; (ii) thiosemicarbazide, conc. HCl/absolute ethanol, reflux, 8–12 h

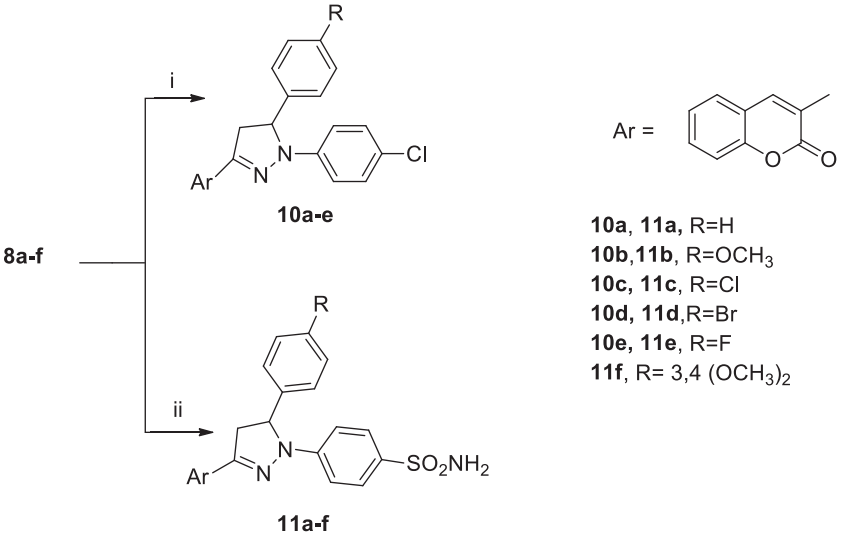

SCHEME 4 Synthesis of the target compounds **10a–e** and **11a–f**. Reagents and conditions: (i) 4-Chlorophenylhydrazine HCl, glacial acetic acid/absolute ethanol, reflux, 8 h; (ii) 4-hydrazinylbenzenesulfonamide HCl, glacial acetic acid/absolute ethanol, reflux, 12 h

exhibited higher activity with IC_{50} range of 0.005–4.120 μM (IC_{50} of erlotinib: 4.700 μM) (Table 1).

The coumarin derivatives carrying pyrazole-1-carbothioamide at position 8 (**9a–f**) exhibited cytotoxicity (IC_{50} range: 0.02–0.99 μM). In series **9a–f**, the substituent at the 5th position of the pyrazoline nucleus markedly affected the activity. The *p*-chlorophenyl derivative **9d** exhibited the greatest activity with IC_{50} 0.02 μM, whereas its bromophenyl isostere **9e** possessed a diminished activity with IC_{50} 0.059 μM. The *p*-fluorophenyl derivative **9f** was the least active one of the 3-halo derivatives with IC_{50} 0.15 μM. Also, the *p*-methoxyphenyl derivative **9b** was the least active analog with IC_{50} 0.99 μM, less active than the phenyl derivative **9a** with IC_{50} 0.37 μM, whereas the *p*-hydroxyphenyl derivative **9c** showed greater activity than its phenyl and the methoxy analogs with IC_{50} 0.061 μM.

However, the series with a *p*-chlorophenyl substituent at position 1 of the pyrazoline nucleus, **10a–e**, exihibited good cytotoxic activity with IC_{50} range 0.42–1.7 μM. The presence of a second *p*-chlorophenyl moiety at the 5th position of the pyrazoline moiety resulted in the most active congener **10c** with IC_{50} 0.42 μM. Its isosteric congener with the *p*-bromophenyl moiety, **10d**, showed diminished activity with IC_{50} 1.1 μM. The six coumarin–pyrazoline hybrids containing benzenesulfonamide moiety, **11a–f**, showed cytotoxic activity with IC_{50} range 0.4–8.3 μM. Two derivatives, **11a** with IC_{50} 0.68 μM and **11c** with IC_{50} 0.4 μM, were more potent than the standard drug. The most active compound was **11c**, which carries the *p*-chlorophenyl moiety in the 5th position of the pyrazoline

TABLE 1 The IC_{50} (μM) values of the new synthesized coumarin derivatives against MCF-7 cells

Compound	IC_{50} (μM)
9a	0.370
9b	0.990
9c	0.061
9d	0.021
9e	0.059
9f	0.150
10a	0.910
10b	1.620
10c	0.420
10d	1.100
10e	1.700
11a	0.680
11b	1.010
11c	0.400
11d	8.300
11e	1.810
11f	1.400
Doxorubicin	0.800
Erlotinib	4.670

Note: Results were obtained from the mean of measurements of three different experiments.

TABLE 2 The IC_{50} values of the most active compound **9d** against the HCT-116, HepG-2, A549, and SGC-7901 cell lines

	Cell line; IC_{50} values (μM)			
Compound	Colon (HCT-116)	Liver (HepG-2)	Lung (A549)	Gastric cancer cell (SGC-7901)
9d	0.021	0.170	0.028	0.110
Doxorubicin	4.430	3.310	2.020	6.350
Erlotinib	2.820	3.900	3.110	20.350

Note: Results were obtained from the mean of measurements of three different experiments.

nucleus. Replacement of this moiety with the isosteric group *p*-bromophenyl **11d** greatly decreased the cytotoxic activity with IC_{50} 8.3 μM.

The most active compound **9d** was further tested against the HCT-116, HepG-2, A549, and SGC-7901 cell lines by MTT assay, and it showed very potent activity against the four tested cell lines. It was more potent than the reference drugs.

2.2.2 | In vitro inhibition of EGFR expression level

The most active derivative **9d** was tested for its ability to inhibit EGFR expression levels, utilizing breast cancer cell line MCF-7 obtained from American Type Culture Collection, with erlotinib as a reference drug.[46,47] The tested compound showed comparable activity to that of erlotinib (Table 3).

2.3 | Molecular docking

Docking was performed to investigate the possibility of direct interactions between the new coumarin derivatives, **9a**–**f**, **10a**–**e**, and **11a**–**f**, and the EGFR TK. For each compound, eight conformers were randomly generated and separately docked into the ATP-binding site of the enzyme. Clustering analysis was performed on the resulting poses and the highest populated clusters were identified. From these highly populated clusters, poses with the highest scores are provided in Table 4. The co-crystallized ligand, erlotinib, was also docked starting from a two-dimensional structure and using the same protocol for preparation and analysis. The score from this self-docking is also included in Table 4. As illustrated in Figure 2, the pose for erlotinib was accurately predicted; however, the docking algorithm does not consider explicit water molecules. As given in Table 4, the predicted scores for the coumarin series are either similar to or better than that of the self-docked erlotinib. It is known that erlotinib interacts with the gatekeeper threonine via a water-bridged hydrogen bond. This is not duly counted by the scoring function, and thus the docking score for erlotinib might be underestimated.

Studying the predicted binding poses of the coumarin derivatives further favors their hypothesized direct inhibitory role. The majority of poses have the coumarin ring forming a hydrogen bond with the backbone atom of Met769 in the hinge region. As depicted in Figure 3, the carbonyl of the coumarin ring nearly overlaps with the nitrogen of the quinazoline ring of erlotinib, which equivalently serves to bind to Met769. The dihydropyrazol ring positions substituents at 1 and 5 to further interact with the Thr766 gatekeeper and the activation loop, respectively. Interestingly, the phenyl ring at position 5 is off the plane of the coumarin ring by an angle which

TABLE 3 EGFR inhibitory activity of the most active synthesized compound

Compound no.	% Inhibition of EGFR
9d	87.00
Erlotinib	95.68

Abbreviation: EGFR, epidermal growth factor receptor.

TABLE 4 Scoring results of the new coumarin derivatives in the active site of EGFR TK (PDB ID: 1M17)

Ligand	Docking score
9a	−8.2
9b	−8.2
9c	−7.9
9d	−8.0
9e	−8.4
9f	−7.9
10a	−10.0
10b	−9.9
10c	−9.0
10d	−9.8
10e	−10.1
11a	−9.6
11b	−9.6
11c	−10.2
11d	−10.1
11e	−9.6
11f	−10
Erlotinib	−7.8

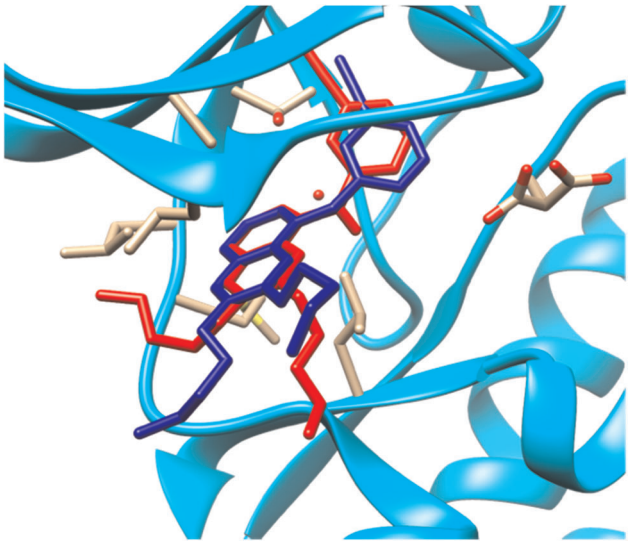

FIGURE 2 Illustration of the overlap between the predicted pose of erlotinib (red) and the actual co-crystallized pose (blue)

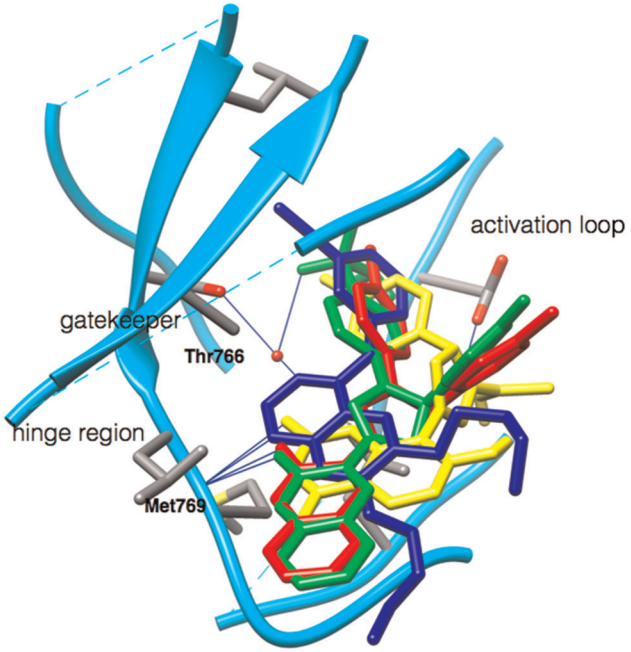

FIGURE 3 The docked poses of the coumarin representatives: **9d** (yellow), **10c** (red), and **11c** (green) along with the co-crystallized erlotinib (blue) in the ATP-binding site of the epidermal growth factor receptor tyrosine kinase. Hydrogen bonds are shown as blue lines

makes it occupy the same region as the ethynyl-phenyl in erlotinib, as shown in Figure 3.

2.4 | ADME (absorption, distribution, metabolism, and excretion) properties

To understand the pharmacokinetic behavior of the most active compounds from each class of the newly synthesized compounds **9d**, **9e**, **10c**, and **11c**, ADME calculations were performed using swissadme.che platform. The obtained results are summarized in Table 5.

According to the analysis of this table, we can assume that most of the active drugs follow druglikeness behavior with moderate water solubility, high gastrointestinal (GI) absorption, and no blood–brain barrier passing except for compound **10c**. These results can represent a step toward further investigations.

3 | CONCLUSION

Novel series of coumarin–pyrazoline hybrids **9a–f**, **10a–e**, and **11a–f** were synthesized and evaluated for their anticancer activity. All the synthesized compounds demonstrated potent activity against the MCF-7 cell line. The most active compound **9d** was further tested against HCT-116, HepG-2, A549, and SGC-7901 cell lines and showed very potent activity against the four tested cell lines, even more than the reference standard, doxorubicin. Compound **9d** possessed superior activity at low nanomolar levels, with IC_{50} 21 nM, against HCT-116. The most active compound **9d** was studied for its ability to inhibit EGFR expression levels where the percent reduction in EGFR reached 87%. On the molecular level, our docking study predicts favorable binding poses between our new compounds and the EGFR TK, suggesting that their antitumor mechanism might involve direct inhibition.

4 | EXPERIMENTAL

4.1 | Chemistry

4.1.1 | General

Unless otherwise noted, all materials were obtained from commercial suppliers and used without further purification. Reactions were monitored on FLUKA silica gel thin-layer chromatography (TLC) aluminum cards (0.2 mm thickness) with fluorescent indicator 254 nm using chloroform/methanol (9.5:0.5) as an eluent. Melting points were determined on Electrothermal 9100 melting point apparatus and were uncorrected. Elemental microanalyses were performed at the Regional Center for Microbiology and Biotechnology, Al-Azhar University. NMR spectra were recorded on Bruker spectrometer at 400 MHz for ^{1}H NMR and at 100 MHz for ^{13}C NMR, and on Varian mercury 300BB at 300 MHz for ^{1}H NMR and at 75.45 MHz for ^{13}C NMR, using tetramethylsilane as the internal reference. Chemical shift values were given in ppm. Mass spectra were performed on Finnigan MAT, SSQ 7000 mass spectrophotometer at 70 eV. Infrared spectra (IR) were recorded on Shimadzu FT-IR 8400S spectrophotometer (Shimadzu) and expressed in wavenumber (cm^{-1}), using potassium bromide discs.

TABLE 5 ADME properties of compounds **9d**, **9e**, **10c**, and **11c**

Compound no.	Log *P* (lipophilicity)	Log *S* (water solubility)	GI absorption	BBB passing	Lipinski's violation	Druglikeness
9d	3.54	Moderate	High	No	0	Yes
9e	3.56	Moderate	High	No	0	Yes
10c	5.39	Poorly	High	Yes	1	Yes
11c	3.77	Moderate	High	No	0	Yes

Abbreviation: ADME, absorption, distribution, metabolism, and excretion; BBB, blood–brain barrier; GI, gastrointestinal.

The InChI codes of the investigated compounds, together with some biological activity data, are provided as Supporting Information.

*7-Hydroxy-4-methyl-2H-chromen-2-one (**2**)*

Compound **2** was prepared according to the literature procedure.[38]

*4-Methyl-2-oxo-2H-chromen-7-yl acetate (**3**)*

Compound **3** was prepared according to the literature procedure.[39]

*8-Acetyl-7-hydroxy-4-methyl-2H-chromen-2-one (**4**)*

Compound **4** was prepared according to the literature procedure.[40]

*3-Acetyl-2H-chromen-2-one (**6**)*

Compound **6** was prepared according to the literature procedure.[41]

4.1.2 | General procedure for the synthesis of 7-hydroxy-4-methyl-8-(arylacryloyl)-2*H*-chromen-2-one (**7a–f**)

Compounds of this series (**7a–f**) were prepared according to the literature procedure.[42]

4.1.3 | General procedure for the synthesis of 3-(arylacryloyl)-2*H*-chromen-2-one (**8a–f**)

Compounds of this series (**8a–f**) were prepared according to the literature procedure.[43]

4.1.4 | General procedure for the synthesis of 3-(7-hydroxy-4-methyl-2-oxo-2*H*-chromen-8-yl)-5-(4-(un)substituted phenyl)-4,5-dihydro-1*H*-pyrazole-1-carbothioamide (**9a–f**)

A mixture of the appropriate chalcones **7a–f** (10 mmol), thiosemicarbazide (0.91 g, 10 mmol), and concentrated hydrochloric acid (1 ml) was refluxed in ethanol for 8 h (TLC). The precipitate obtained was collected, dried, and crystallized from dimethylformamide/ethanol.

*3-(7-Hydroxy-4-methyl-2-oxo-2H-chromen-8-yl)-5-phenyl-4,5-dihydro-1H-pyrazole-1-carbothioamide (**9a**)*

Yield: 80%, m.p. 239–241°C. IR υmax (cm^{-1}): 3420 (OH), 3265, 3170 (CH aliphatic), 1730 (C=O), 1602, 1510 (C=C, C=N), 1220 (C=S). ^{1}H NMR (dimethyl sulfoxide (DMSO)-d_6-400 MHz) δ ppm: 2.45 (s, 3H, CH_3), 2.91 (dd, 1H, C4-H_B pyrazoline, J_{BX} = 11.9 Hz, J_{BA} = 16.8 Hz), 3.66 (dd, 1H, C4-H_A pyrazoline, J_{AX} = 2.8 Hz, J_{AB} = 16.8 Hz), 5.40 (dd, 1H, C5-H_X pyrazoline, J_{XA} = 2.8 Hz, J_{XB} = 11.9 Hz), 6.34 (s, 1H, C3-H chromene), 7.07 (d, 1H, C5-H, *J* = 8.6 Hz), 7.30 (t, 3H, Ar-H, *J* = 8.8 Hz), 7.60 (d, 2H, Ar-H, *J* = 8.6 Hz), 7.82 (m, 2H, C6-H chromene + SH, D_2O exch.), 8.64 (s, 1H, NH, D_2O exch.), 11.01 (s, 1H, OH, D_2O exch.). Anal. calculated for $C_{20}H_{17}N_3O_3S$ (379.43): C, 63.31; H, 4.52; N, 11.07. Found: C, 63.57; H, 4.58; N, 11.22. Mass spectrometry (MS): *m/z* 379.1, M+ (16.37%), 284.97 (100%).

*3-(7-Hydroxy-4-methyl-2-oxo-2H-chromen-8-yl)-5-(4-methoxyphenyl)-4,5-dihydro-1H-pyrazole-1-carbothioamide (**9b**)*

Yield: 92%, m.p. 270–272°C. IR υmax (cm^{-1}): 3420 (OH), 2927 (CH aliphatic), 1730 (C=O), 1602, 1510 (C=C, C=N), 1200 (C=S). ^{1}H NMR (DMSO-d_6-400 MHz) δ ppm: 2.40 (s, 3H, CH_3), 3.18 (dd, 1H, C4-H_A pyrazoline, J_{AX} = 3.2 Hz, J_{AB} = 18.5 Hz), 3.74 (OCH_3), 4.02 (dd, 1H, C4-H_B pyrazoline, J_{BX} = 11.5 Hz, J_{BA} = 18.5 Hz), 5.88 (dd, 1H, C5-H_X pyrazoline, J_{XA} = 3.2 Hz, J_{XB} = 11.5 Hz), 6.22 (s, 1H, C3-H chromene), 6.88 (d, 2H, Ar–H, *J* = 8.6 Hz), 6.99 (d, 1H, C5-H chromene, *J* = 8.8 Hz), 7.22 (d, 2H, Ar–H, *J* = 8.6 Hz), 7.72 (d, 1H, C6-H chromene + SH, D_2O exch.), 7.99 (s, 1H, NH, D_2O exch.), 11.04 (s, 1H, OH, D_2O exch.). ^{13}C NMR (DMSO-d_6): δ 18.83 (CH_3), 46.75 (C-4 pyrazoline), 55.50 (OCH_3), 61.94 (C-5 pyrazoline), 106.46, 111.01, 112.71, 113.47, 114.20, 127.60, 128.26, 135.40, 152.92, 153.24, 154.14 (aromatic C), 158.75, 159.81, 160.07, 176.66 (C7 chromene, carbonyl and C=S). Anal. calculated for $C_{21}H_{19}N_3O_4S$ (409.46): C, 61.60; H, 4.68; N, 10.26. Found: C, 61.76; H, 4.73; N, 10.39.

*3-(7-Hydroxy-4-methyl-2-oxo-2H-chromen-8-yl)-5-(4-hydroxyphenyl)-4,5-dihydro-1H-pyrazole-1-carbothioamide (**9c**)*

Yield: 80%, m.p. 244–246°C. IR υmax (cm^{-1}): 3420 (OH), 3265, 3170 (NH_2), 2927 (CH aliphatic), 1730 (C=O), 1600, 1480 (C=C, C=N), 1200 (C=S). ^{1}H NMR (DMSO-d_6-400 MHz) δ ppm: 2.41 (s, 3H, CH_3), 3.24 (dd, 1H, C4-H_B pyrazoline, J_{BX} = 12.2 Hz, J_{BA} = 16.3 Hz), 3.58 (dd, 1H, C4-H_A pyrazoline, J_{AX} = 3.0 Hz, J_{AB} = 16.8 Hz), 5.30 (dd, 1H, C5-H_X pyrazoline, J_{XA} = 2.8 Hz, J_{XB} = 11.4 Hz), 6.85 (d, 2H, Ar–H, *J* = 8.1 Hz), 6.9 (s, 1H, C3-H chromene), 7.11 (d, 2H, Ar–H, *J* = 8.1 Hz), 7.43 (d, 1H, C5-H chromene, *J* = 8.7 Hz), 7.80 (d, 1H, C6-H chromene, *J* = 8.7 Hz), 8.3 (s, 2H, NH_2, D_2O exch.), 10.9 (s, 1H, OH, D_2O exch.). Anal. calculated for $C_{20}H_{17}N_3O_4S$ (395.43): C, 60.75; H, 4.33; N, 10.63. Found: C, 60.91; H, 4.39; N, 10.78. MS: *m/z* 395.47, M+, 105 (100%).

*5-(4-Chlorophenyl)-3-(7-hydroxy-4-methyl-2-oxo-2H-chromen-8-yl)-4,5-dihydro-1H-pyrazole-1-carbothioamide (**9d**)*

Yield: 80%, m.p. 265–267°C. IR υmax (cm^{-1}): 3420 (OH), 3265, 3170 (NH_2), 2927 (CH aliphatic), 1730 (C=O), 1602, 1508 (C=C, C=N), 1200 (C=S). ^{1}H NMR (DMSO-d_6-400 MHz), δ ppm: 2.50 (s, 3H, CH_3), 2.88 (dd, 1H, C4-H_B pyrazoline, J_{BX} = 12.0 Hz, J_{BA} = 16.8 Hz), 3.62 (dd, 1H, C4-H_A pyrazoline, J_{AX} = 2.8 Hz, J_{AB} = 16.8 Hz), 5.37 (dd, 1H, C5-H_X pyrazoline, J_{XA} = 2.8 Hz, J_{XB} = 12.0 Hz), 6.31 (s, 1H, C3-H chromene), 7.05 (d, 1H, C5-H chromene, *J* = 8.6 Hz), 7.28 (d, 2H, Ar–H, *J* = 8.3 Hz), 7.60 (d, 2H, Ar–H, *J* = 8.3 Hz), 7.73 (m, 2H, C6-H chromene + SH, D_2O exch.), 8.6 (s, 1H, NH, D_2O exch.), 10.84 (s, 1H, OH, D_2O exch.). Anal. calculated for $C_{20}H_{16}ClN_3O_3S$ (378.88): C, 58.04; H, 3.90; N, 10.15. Found: C, 58.12; H, 3.87; N, 10.31.

*5-(4-Bromophenyl)-3-(7-hydroxy-4-methyl-2-oxo-2H-chromen-8-yl)-4,5-dihydro-1H-pyrazole-1-carbothioamide (**9e**)*

Yield: 80%, m.p. 270–273°C. IR υmax (cm^{-1}): 3420 (OH), 3265, 3170 (NH_2), 2927 (CH aliphatic), 1730 (C=O), 1602, 1510 (C=C, C=N), 1200 (C=S). ^1H NMR (DMSO-d_6 400 MHz), δ ppm: 2.50 (s, 3H, CH_3), 2.89 (dd, 1H, C4-H_B pyrazoline, J_{BX} = 11.8 Hz, J_{BA} = 16.7 Hz), 4.01 (dd, 1H, C4-H_A pyrazoline, J_{AX} = 2.8 Hz, J_{AB} = 16.7 Hz), 5.40 (dd, 1H, C5-H_X pyrazoline, J_{XA} = 2.8 Hz, J_{XB} = 11.8 Hz), 6.32 (s, 1H, C3-H chromene), 7.06 (d, 1H, C5-H chromene, *J* = 8.8 Hz), 7.52 (d, 2H, Ar–H, *J* = 8.5 Hz), 7.58 (d, 2H, Ar–H, *J* = 8.5 Hz), 7.75 (d, 1H, C6-H chromene, *J* = 8.8 Hz), 8.61 (s, 2H, NH_2, D_2O exch.), 10.85 (s, 1H, OH, D_2O exch.). ^{13}C NMR (DMSO-d_6): δ 19.15 (CH_3), 31.86 (C-4 pyrazoline), 76.14 (C-5 pyrazoline), 108.72, 111.70, 114.68, 114.67, 128.98, 131.86, 138.85, 138.87, 139.56, 151.78, 154.41 (aromatic C), 160.32, 160.38 (C7 chromene and carbonyl), 180.07 (C=S). Anal. calculated for $C_{20}H_{16}BrN_3O_3S$ (458.33): C, 52.41; H, 3.52; N, 9.17. Found: C, 52.49; H, 3.5; N, 9.26.

*5-(4-Fluorophenyl)-3-(7-hydroxy-4-methyl-2-oxo-2H-chromen-8-yl)-4,5-dihydro-1H-pyrazole-1-carbothioamide (**9f**)*

Yield: 75%, m.p. 241–243°C. IR υmax (cm^{-1}): 3420 (OH), 3265, 3170 (NH_2), 2927 (CH aliphatic), 1730 (C=O), 1602, 1510 (C=C, C=N), 1200 (C=S). ^1H NMR (DMSO-d_6-400 MHz) δ ppm: 2.50 (s, 3H, CH_3), 2.89 (dd, 1H, C4-H_B pyrazoline, J_{BX} = 11.7 Hz, J_{BA} = 16.4 Hz), 3.67 (dd, 1H, C4-H_A pyrazoline, J_{AX} = 3.0 Hz, J_{AB} = 16.4 Hz), 5.41 (dd, 1H, C5-H_X pyrazoline, J_{XA} = 3.0 Hz, J_{XB} = 11.7 Hz), 6.34 (s, 1H, C3-H chromene), 7.08 (d, 1H, C5-H chromene, *J* = 8.8 Hz), 7.53 (d, 2H, Ar–H, *J* = 8.4 Hz), 7.67 (d, 2H, Ar–H, *J* = 8.4 Hz), 7.75 (d, 1H, C6-H chromene, *J* = 8.8 Hz), 8.64 (s, 2H, NH_2, D_2O exch.), 10.88 (s, 1H, OH, D_2O exch.). ^{13}C NMR (DMSO-d_6): δ 19.15 (CH_3), 32.08 (C-4 pyrazoline), 76.29 (C-5 pyrazoline), 108.75, 111.69, 114.71, 114.76, 115.77 (d, $^2J_{F-c}$ = 22 Hz), 127.64, 129.09 (d, $^3J_{F-c}$ = 8 Hz), 135.70, 151.84, 154.47 (aromatic C), 160.43, 160.52 (C7 chromene and carbonyl), 162.48 (d, $^1J_{F-c}$ = 247 Hz), 180.08 (C=S). Anal. calculated for $C_{20}H_{16}FN_3O_3S$ (397.42): C, 60.44; H, 4.06; N, 10.57. Found: C, 60.57; H, 4.11; N, 10.69.

4.1.5 | General procedure for the synthesis of 3-(1-(4-chlorophenyl)-5-(4-un(substituted)phenyl)-4,5-dihydro-1*H*-pyrazol-3-yl)-2*H*-chromen-2-one (**10a–e**)

To a solution of the appropriate chalcones **8a–e** (10 mmol), 4-chlorophenylhydrazine (1.72 g, 10 mmol) was added in absolute ethanol (30 ml) in the presence of glacial acetic acid (1 ml) and refluxed for 8 h. The reaction mixture was filtered while hot, left to dry, and crystallized from acetonitrile.

*3-(1-(4-Chlorophenyl)-5-phenyl-4,5-dihydro-1H-pyrazol-3-yl)-2H-chromen-2-one (**10a**)*

Yield: 83%, m.p. 202–204°C. IR υmax (cm^{-1}): 2933 (CH aliphatic), 1726 (C=O), 1602, 1510 (C=C, C=N). ^1H NMR (DMSO-400 MHz), δ ppm: 3.24 (dd, 1H, C4-H_A pyrazoline, J_{AX} = 5.96 Hz, J_{AB} = 17.96 Hz), 4.01 (dd, 1H, C4-H_B pyrazoline, J_{BX} = 12.4 Hz, J_{BA} = 17.96 Hz), 5.55 (dd, 1H, C5-H_X pyrazoline, J_{XA} = 5.96 Hz, J_{XB} = 12.4 Hz), 7.03 (d, 2H, Ar–H, *J* = 9.0 Hz), 7.22 (d, 2H, Ar–H, *J* = 9.0 Hz), 7.27 (t, 3H, Ar–H, *J* = 7.56 Hz), 7.34–7.42 (m, 4H, C5-H chromene, C6-H chromene and Ar–H), 7.61 (t, 1H, C7-H chromene, *J* = 7.8 Hz), 7.82 (d, 1H, C8-H chromene, *J* = 7.76 Hz), 8.50 (s, 1H, C4-H chromene). ^{13}C NMR (DMSO-100.63 MHz): 45.16 (C-4 pyrazoline), 63.38 (C-5 pyrazoline), 115.12, 116.36, 119.59, 120.15, 123.29, 125.24, 126.21, 128.07, 129.29, 129.55, 132.50, 139.43, 142.21, 142.82, 144.58, 153.44, (aromatic C), 158.52 (carbonyl). Anal. calculated for $C_{24}H_{17}ClN_2O_2$ (400.86): C, 71.91; H, 4.27; N, 6.99. Found: C, 72.13; H, 4.35; N, 7.12.

*3-(1-(4-Chlorophenyl)-5-(4-methoxyphenyl)-4,5-dihydro-1H-pyrazol-3-yl)-2H-chromen-2-one (**10b**)*

Yield: 89%, m.p. 219–222°C. IR υmax (cm^{-1}): 3352, 3181 (NH_2), 2932 (CH aliphatic), 1729 (C=O), 1659, 1533 (C=C, C=N). ^1H NMR (DMSO-400 MHz), δ ppm: 3.21 (dd, 1H, C4-H_A pyrazoline, J_{AX} = 5.1 Hz, J_{AB} = 18.2 Hz), 3.71 (s, 3H, OCH_3), 3.96 (dd, 1H, C4-H_B pyrazoline, J_{BX} = 12.2 Hz, J_{BA} = 18.2 Hz), 5.49 (dd, 1H, C5-H_X pyrazoline, J_{XA} = 5.1 Hz, J_{XB} = 12.2 Hz), 6.88 (d, 2H, Ar–H, *J* = 8.6 Hz), 7.04 (d, 2H, Ar–H, *J* = 8.96 Hz), 7.18 (d, 2H, Ar–H, *J* = 8.6 Hz), 7.24 (d, 2H, Ar–H, *J* = 8.96 Hz), 7.35–7.42 (m, 2H, C5-H chromene and C6-H chromene), 7.61 (t, 1H, C7-H chromene, *J* = 8.1 Hz), 7.82 (d, 1H, C8-H chromene, *J* = 7.7 Hz), 8.48 (s, 1H, C4-H chromene). ^{13}C NMR (DMSO-100.63 MHz): 45.15 (C-4 pyrazoline), 55.50 (OCH_3), 62.95 (C-5 pyrazoline), 114.87, 115.19, 116.35, 119.34, 120.22, 123.42, 125.21, 127.48, 129.13, 132.43, 134.01, 139.27, 141.72, 142.71, 144.53, 153.42, 158.53 (aromatic C), 159.53 (carbonyl). Anal. calculated for $C_{25}H_{19}ClN_2O_3$ (430.88): C, 69.69; H, 4.44; N, 6.50. Found: C, 69.85; H, 4.49; N, 6.59. MS: *m/z* 430.10, M+, 110 (100%).

*3-(1,5-Bis(4-chlorophenyl)-4,5-dihydro-1H-pyrazol-3-yl)-2H-chromen-2-one (**10c**)*

Yield: 83%, m.p. 182–184°C. IR υmax (cm^{-1}): 2933 (CH aliphatic), 1726 (C=O), 1602, 1495 (C=C, C=N). ^1H NMR (DMSO-400 MHz), δ ppm: 3.23 (dd, 1H, C4-H_A pyrazoline, J_{AX} = 5.8 Hz, J_{AB} = 18.0 Hz), 4.0 (dd, 1H, C4-H_B pyrazoline, J_{BX} = 12.4 Hz, J_{BA} = 18.0 Hz), 5.58 (dd, 1H, C5-H_X pyrazoline, J_{XA} = 5.8 Hz, J_{XB} = 12.4 Hz), 7.02 (d, 2H, Ar–H, *J* = 8.96 Hz), 7.21 (d, 2H, Ar–H, *J* = 8.4 Hz), 7.28 (d, 2H, Ar–H, *J* = 8.4 Hz), 7.36 (d, 1H, C5-H chromene, *J* = 7.7 Hz), 7.40–7.45 (m, 3H, Ar–H and C6-H chromene), 7.65 (t, 1H, C7-H chromene, *J* = 7.5 Hz), 7.82 (d, 1H, C8-H chromene, *J* = 7.7 Hz), 8.49 (s, 1H, C4-H chromene). Anal. calculated for $C_{24}H_{16}Cl_2N_2O_2$ (435.30): C, 66.22; H, 3.70; N, 6.44. Found: C, 66.40; H, 3.67; N, 6.85. MS: *m/z* 435.80, 437.66, M+ (3:1 ratio), 107.05 (100%).

*3-(5-(4-Bromophenyl)-1-(4-chlorophenyl)-4,5-dihydro-1H-pyrazol-3-yl)-2H-chromen-2-one (**10d**)*

Yield: 83%, m.p. 188–190°C. IR υmax (cm^{-1}): 2933 (CH aliphatic), 1726 (C=O), 1602, 1495 (C=C, C=N). ^1H NMR (DMSO-400 MHz), δ ppm: 3.23 (dd, 1H, C4-H_A pyrazoline, J_{AX} = 5.76 Hz, J_{AB} = 18.04 Hz), 4.00 (dd, 1H, C4-H_B pyrazoline, J_{BX} = 12.4 Hz, J_{BA} = 18.04 Hz), 5.56 (dd, 1H, C5-H_X pyrazoline, J_{XA} = 5.76 Hz, J_{XB} = 12.4 Hz), 7.01 (d, 2H,

Ar–H, *J* = 8.92 Hz), 7.21 (d, 2H, Ar–H, *J* = 8.7 Hz), 7.22 (d, 2H, Ar–H, *J* = 8.92 Hz), 7.39 (d, 2H, Ar–H, *J* = 8.7 Hz), 7.52 (m, 2H, C5-H chromene and C6-H chromene), 7.62 (t, 1H, C7-H chromene, *J* = 7.5 Hz), 7.81 (d, 1H, C8-H chromene, *J* = 7.7 Hz), 8.49 (s, 1H, C4-H chromene). Anal. calculated for $C_{24}H_{16}BrClN_2O_2$ (479.7): C, 60.08; H, 3.36; N, 5.84. Found: C, 60.29; H, 3.40; N, 5.91.

*3-(1-(4-Chlorophenyl)-5-(4-fluorophenyl)-4,5-dihydro-1H-pyrazol-3-yl)-2H-chromen-2-one (**10e**)*

Yield: 83%, m.p. 178–180°C. IR υmax (cm^{-1}): 2933 (CH aliphatic), 1726 (C=O chromene), 1602, 1495 (C=C, C=N). ^{1}H NMR (DMSO-400 MHz), δ ppm: 3.23 (dd, 1H, C4-H_A pyrazoline, J_{AX} = 5.8 Hz, J_{AB} = 18.0 Hz), 4.00 (dd, 1H, C4-H_B pyrazoline, J_{BX} = 12.3 Hz, J_{BA} = 18.0 Hz), 5.58 (dd, 1H, C5-H_X pyrazoline, J_{XA} = 5.8 Hz, J_{XB} = 12.3 Hz), 7.40 (d, 2H, Ar–H, *J* = 8.8 Hz), 7.03 (d, 2H, Ar–H, *J* = 8.8 Hz), 7.17 (d, 2H, Ar–H, *J* = 8.8 Hz), 7.23 (d, 2H, Ar–H, *J* = 8.96 Hz), 7.37 (d, 1H, C5-H chromene, *J* = 7.5 Hz), 7.47 (t, 1H, C6-H chromene, *J* = 7.4 Hz), 7.62 (t, 1H, C7-H chromene, *J* = 7.2 Hz), 7.82 (d, 1H, C8-H chromene, *J* = 7.5 Hz), 8.50 (s, 1H, C4-H chromene). ^{13}C NMR (DMSO-100.63 MHz): 45.07 (C-4 pyrazoline), 62.63 (C-5 pyrazoline), 115.17, 115.81 (d, $^2J_{F\text{-}c}$ = 22 Hz), 119.59, 120.14, 122.12, 123.39, 125.27, 128.36 (d, $^3J_{F\text{-}c}$ = 8 Hz), 129.24, 132.55, 138.32, 139.55, 141.59, 142.71, 144.68, 153.46, (aromatic C), 158.53 (carbonyl). 161.90 (d, $^1J_{F\text{-}c}$ = 242 Hz); Anal. calculated for $C_{24}H_{16}ClFN_2O_2$ (418.85): C, 68.82; H, 3.85; N, 6.69. Found: C, 68.97; H, 3.94; N, 6.82.

4.1.6 | General procedure for the synthesis of 4-(3-(2-oxo-2*H*-chromen-3-yl)-5-(3,4-(un)substituted phenyl)-4,5-dihydro-1*H*-pyrazol-1-yl) benzenesulfonamide (**11a–e**)

4-Hydrazinylbenzenesulfonamide (1.72 g, 10 mmol) was added to a solution of the appropriate chalcone derivatives **8a–e** (2.50 g, 10 mmol) in absolute ethanol (30 ml) in the presence of glacial acetic acid (1 ml) and heated under reflux for 12 h. The reaction mixture was filtered while hot. The obtained solid was dried and crystallized from acetonitrile.

*4-(3-(2-Oxo-2H-chromen-3-yl)-5-phenyl-4,5-dihydro-1H-pyrazol-1-yl)benzenesulfonamide (**11a**)*

Yield: 73%, m.p. 200–203°C. IR υmax (cm^{-1}): 3249, 3170 (NH_2), 2927 (CH aliphatic), 1728 (C=O), 1596, 1536 (C=C, C=N), 1304, 1078 (SO_2). ^{1}H NMR (DMSO-d_6-400 MHz, δ ppm): 3.30 (dd, 1H, C4-H_A pyrazoline, J_{AX} = 4.7 Hz, J_{AB} = 18.1 Hz), 4.05 (dd, 1H, C4-H_B pyrazoline, J_{BX} = 12.2 Hz, J_{BA} = 18.1 Hz), 5.82 (dd, 1H, C5-H_X pyrazoline, J_{XA} = 4.7 Hz, J_{XB} = 12.2 Hz), 7.06 (s, 2H, NH_2, D_2O exch.), 7.14 (d, 2H, Ar–H, *J* = 8.6 Hz), 7.32 (t, 3H, Ar–H, *J* = 8.6 Hz), 7.44 (m, 2H, C5-H chromene and C6-H chromene), 7.55 (d, 2H, Ar–H, *J* = 8.3 Hz), 7.36–7.45 (m, 3H, Ar–H and C7-H chromene), 7.82 (d, 1H, C8-H chromene, *J* = 8.8 Hz), 8.55 (s, 1H, C4-H chromene). Anal. calculated for $C_{24}H_{19}N_3O_4S$ (445.49): C, 64.71; H, 4.30; N, 9.43. Found: C, 64.97; H, 4.39; N, 9.58. MS: m/z 445.1, M^+, 77 (100%).

*4-(5-(4-Methoxyphenyl)-3-(2-oxo-2H-chromen-3-yl)-4,5-dihydro-1H-pyrazol-1-yl)benzenesulfonamide (**11b**)*

Yield: 89%, m.p. 222–224°C. IR υmax (cm^{-1}): 3352, 3181(NH_2), 2932 (CH aliphatic), 1729 (C=O chromene), 1599, 1533 (C=C, C=N), 1303, 1145 (SO_2). ^{1}H NMR (DMSO-d_6-400 MHz), δ ppm: 3.27 (dd, 1H, C4-H_A pyrazoline, J_{AX} = 5.1 Hz, J_{AB} = 18.1 Hz), 3.71 (s, 3H, OCH_3), 4.00 (dd, 1H, C4-H_B pyrazoline, J_{BX} = 12.2 Hz, J_{BA} = 18.1 Hz), 5.62 (dd, 1H, C5-H_X pyrazoline, J_{XA} = 5.1 Hz, J_{XB} = 12.2 Hz), 6.90 (d, 2H, Ar–H, *J* = 8.8 Hz), 7.06 (s, 2H, NH_2, D_2O exch.), 7.13 (d, 2H, Ar–H, *J* = 8.7 Hz), 7.18 (d, 2H, Ar–H, *J* = 8.7 Hz), 7.40–7.44 (m, 2H, C5-H chromene and C6-H chromene), 7.61 (d, 2H, Ar–H, *J* = 8.9 Hz), 7.60 (t, 1H, C7-H chromene, *J* = 8.44 Hz), 7.81 (d, 1H, C8-H chromene, *J* = 7.3 Hz), 8.56 (s, 1H, C4-H chromene). ^{13}C NMR (DMSO-100.63 MHz): 45.09 (C-4 pyrazoline), 55.52 (OCH_3), 62.32 (C-5 pyrazoline), 112.92, 114.42, 116.43, 119.55, 120.06, 125.31, 127.45, 127.55, 129.42, 132.74, 133.73, 134.15, 140.13, 145.86, 146.22, 153.56, 158.52 (aromatic C), 159.11 (carbonyl). Anal. calculated for $C_{25}H_{21}N_3O_5S$ (475.52): C, 63.15; H, 4.45; N, 8.84. Found: C, 63.36; H, 4.53; N, 8.97.

*4-(5-(4-Chlorophenyl)-3-(2-oxo-2H-chromen-3-yl)-4,5-dihydro-1H-pyrazol-1-yl)benzenesulfonamide (**11c**)*

Yield: 83%, m.p. 189–191°C. IR υmax (cm^{-1}): 3350, 3178 (NH_2), 2933 (CH aliphatic), 1726 (C=O chromene), 1602, 1510 (C=C, C=N), 1292, 1168 (SO_2). ^{1}H NMR (DMSO/D_2O-400 MHz), δ ppm: 3.28 (dd, 1H, C4-H_A pyrazoline, J_{AX} = 5.0 Hz, J_{AB} = 18.1 Hz), 4.04 (dd, 1H, C4-H_B pyrazoline, J_{BX} = 12.3 Hz, J_{BA} = 18.1 Hz), 5.72 (dd, 1H, C5-H_X pyrazoline J_{XA} = 5.0 Hz, J_{XB} = 12.3 Hz), 7.07 (s, 2H, NH_2, D_2O exch.) 7.12 (d, 2H, Ar–H, *J* = 8.6 Hz), 7.28 (d, 2H, Ar–H, *J* = 8.6 Hz), 7.42 (d, 2H, Ar–H, *J* = 8.3 Hz), 7.53–7.59 (m, 2H, C5-H chromene and C6-H chromene), 7.63 (d, 2H, Ar–H, *J* = 8.3 Hz), 7.74 (dd, 1H, C7-H chromene, *J* = 13.6 Hz, *J* = 8.7 Hz), 7.82 (d, 1H, C8-H chromene, *J* = 7.4 Hz), 8.64 (s, 1H, C4-H chromene). Calculated for $C_{24}H_{18}ClN_3O_4S$ (479.94): C, 60.06; H, 3.78; N, 8.76. Found: C, 60.27; H, 3.86; N, 8.95.

*4-(5-(4-Bromophenyl)-3-(2-oxo-2H-chromen-3-yl)-4,5-dihydro-1H-pyrazol-1-yl)benzenesulfonamide (**11d**)*

Yield: 80%, m.p. 210°C. IR υmax (cm^{-1}): 3350, 3178 (NH_2), 2929 (CH aliphatic), 1723 (C=O chromene), 1596, 1566 (C=C, C=N), 1265, 1087 (SO_2). ^{1}H NMR (DMSO-d_6-400MHz), δ ppm: 3.28 (dd, 1H, C4-H_A pyrazoline, J_{AX} = 5.0 Hz, J_{AB} = 18.1 Hz), 4.04 (dd, 1H, C4-H_B pyrazoline, J_{BX} = 12.2 Hz, J_{BA} = 18.1 Hz), 5.70 (dd, 1H, C5-H_X pyrazoline, J_{XA} = 5.0 Hz, J_{XB} = 12.2 Hz), 7.06 (s, 2H, NH_2, D_2O exch.), 7.20 (d, 2H, Ar–H, *J* = 8.8 Hz), 7.22 (d, 2H, Ar–H, *J* = 8.4 Hz), 7.39 (d, 2H, Ar–H, *J* = 7.7 Hz), 7.40–7.44 (m, 2H, C5-H chromene and C6-H chromene), 7.56 (d, 2H, Ar–H, *J* = 8.4 Hz), 7.63 (t, 1H, C7-H chromene, *J* = 7.6 Hz), 7.83 (d, 1H, C8-H chromene, *J* = 7.7 Hz), 8.57 (s, 1H, C4-H chromene). Anal. calculated for $C_{24}H_{18}BrN_3O_4S$ (524.39): C, 54.97; H, 3.46; N, 8.01. Found: C, 55.01; H, 3.54; N, 8.23.

*4-(5-(4-Fluorophenyl)-3-(2-oxo-2H-chromen-3-yl)-4,5-dihydro-1H-pyrazol-1-yl)benzenesulfonamide (**11e**)*

Yield: 85%, m.p. 217–220°C. IR (KBr, cm^{-1}): 3350, 3178 (NH_2), 3049 (CH aromatic), 2929 (CH aliphatic), 1723 (C=O), 1596, 1566 (C=C,

C=N), 1265, 1087 (SO_2). ^{1}H NMR (DMSO-d_6-400 MHz), δ ppm: 3.29 (dd, 1H, C4-H_A pyrazoline, J_{AX} = 5.0 Hz, J_{AB} = 18.1 Hz), 4.04 (dd, 1H, C4-H_B pyrazoline, J_{BX} = 12.3 Hz, J_{BA} = 18.08 Hz), 5.71 (dd, 1H, C5-H_X pyrazoline, J_{XA} = 5.0 Hz, J_{XB} = 12.3 Hz), 7.07 (s, 2H, NH_2, D_2O exch.), 7.13 (d, 2H, Ar–H, *J* = 8.8 Hz), 7.21 (t, 2H, Ar–H, *J* = 8.8 Hz), 7.31 (dd, 2H, Ar–H, *J* = 8.7 Hz, *J* = 5.4 Hz), 7.38–7.44 (m, 2H, C5-H chromene and C6-H chromene), 7.55–7.64 (m, 3H, Ar-H and C7-H chromene), 7.85 (d, 1H, C8-H chromene, *J* = 7.8 Hz), 8.57 (s, 1H, C4-H chromene). ^{13}C NMR (DMSO-100.63 MHz): 45.02 (C-4 pyrazoline), 62.09 (C-5 pyrazoline), 112.91, 116.39 (d, $^2J_{F\text{-}c}$ = 21 Hz), 116.41, 119.29, 120.12, 125.30, 127.74, 128.31 (d, $^3J_{F\text{-}c}$ = 8 Hz), 129.42, 132.77, 134.35, 138.01, 140.24, 145.75, 146.25, 153.38 (aromatic C), 158.50 (carbonyl), 161.94 (d, $^1J_{F\text{-}c}$ = 242 Hz). Anal. calculated for $C_{24}H_{18}FN_3O_4S$ (463.48): C, 62.19; H, 3.91; N, 9.07. Found: C, 62.38; H, 3.89; N, 9.28.

4.2 | Biological evaluation

4.2.1 | MTT assay for in vitro cytotoxic activity

Antiproliferative activity of the target compounds was determined in cells treated with the different concentrations of the tested compounds in comparison with untreated control using MTT assay as follows.

Cells were grown as a monolayer in media supplemented with 10% inactivated fetal bovine serum. The monolayers of 10,000 cells were plated (10^4 cells/well) in a 96-well tissue culture plate and incubated for 24 h at 37°C in a humidified incubator with 5% CO_2 before treatment with the compounds to allow attachment of cell to the plate, except blank wells without cells. Different concentrations of 100, 10, 1.0, 0.1, and 0.01 μM of each compound were tested for cytotoxicity. Tetraplicate wells were prepared for each concentration in addition to cell control (cells only without compounds). Cells were incubated with the tested compounds for 48 h in a CO_2 incubator at 37°C and 5% CO_2. Culture media containing different concentrations of the tested compounds and dead cells were decanted, leaving only viable attached cells in the tissue culture plate. The plate was washed twice with pre-warmed phosphate-buffered saline (PBS). MTT reagent (40 μl) was added to each well including blank and negative control wells. After addition of MTT reagent, the plates were incubated in the dark for 4 h for the reduction of MTT into formazan (purple color) by dehydrogenase activity in mitochondria of viable cells. DMSO (150μl) was added to each well to solubilize the purple crystals of formazan. Absorbance was measured at 570 nm with a microplate reader (ROBONIK™ P2000 ELISA plate reader). The percentage of cell survival was calculated as follows: [(absorbance of sample − absorbance of blank)/(absorbance of control − absorbance of blank)] × 100. The inhibitory concentration 50 (IC_{50}) was calculated by plotting the log molar concentration of the tested compounds against survival rate percent.

4.2.2 | In vitro EGFR expression inhibition assay in MCF-7 cell line

The cells in culture medium were tested with 20 μl of IC_{50} values of the tested compounds or the standard drug doxorubicin dissolved in DMSO, and then they were incubated for 24 h at 37°C in a humidified 5% CO_2 atmosphere. The cells were harvested and homogenates were prepared in saline using a tight pestle homogenizer until complete cell disruption. The kit uses a double-antibody sandwich enzyme-linked immunosorbent assay (ELISA) to analyze the level of human EGFR in samples. A monoclonal antibody for EGFR was precoated on 96-well plates. Standard and test samples were added to the wells, and a biotinylated detection polyclonal antibody from goat, specific for EGFR, was added subsequently, followed by washing with PBS. Avidin–biotin–peroxidase complex was added and unbound conjugates were washed away with PBS buffer. Horseradish peroxidase (HRP) substrate TMB was used to visualize HRP enzymatic reaction. TMB was catalyzed by HRP to produce a blue-colored product that changed to yellow after adding acidic stop solution. The density of yellow is proportional to the human EGFR amount of sample captured in plate. The chroma of color and the concentration of the human EGFR of sample were positively correlated, and the optical density was determined at 451 nm. The level of human EGFR was calculated (pg/ml) as duplicate determinations from the standard curve.

4.3 | Molecular docking

Docking was performed via AutoDock4.[48] The crystal structure of the target TK in complex with erlotinib, PDB ID: 1M17, was prepared using UCSF Chimera[49] and AutoDock tools.[48] Gasteiger charges were used for the protein and all ligands. A grid box of dimensions 42 × 40 × 40 grid points and spacing 0.375 was centered on erlotinib. For each docking, 100 steps of genetic algorithm were run while keeping all the default settings provided by AutoDock Tools. Eight conformers were generated for each ligand using OpenBabel.[50]

4.4 | ADME properties

The properties were calculated through swissadme.che platfrom.[51] Log *P* values were obtained as consensus log *P* o/w. Log *S* (ESOL) was used to represent water solubility. GI absorption was represented according to BOILED-Egg.[52] Druglikeness was according to Lipinski's rule.[53]

CONFLICTS OF INTERESTS

The authors declare that there are no conflicts of interests.

ORCID

Samar H. Fahim http://orcid.org/0000-0002-7898-6928

REFERENCES

[1] D. Sloane, in Cancer Epidemiology (Ed: M. Verma), Humana Press **2009**, Vol. 471, pp. 65–83.
[2] E. Zwick, J. Bange, A. Ullrich, *Endocr. Relat. Cancer* **2001**, *8*, 161.
[3] T. N. Aung, Z. Qu, R. D. Kortschak, D. L. Adelson, *Int. J. Mol. Sci.* **2017**, *18*, 656.
[4] J. Bronikowska, E. Szliszka, D. Jaworska, Z. P. Czuba, W. Krol, *Molecules* **2012**, *17*, 6449.
[5] T. Devji, C. Reddy, C. Woo, S. Awale, S. Kadota, D. Carrico-Moniz, *Bioorg. Med. Chem. Lett.* **2011**, *21*, 5770.
[6] M. Joao Matos, S. Vazquez-Rodriguez, L. Santana, E. Uriarte, C. Fuentes-Edfuf, Y. Santos, A. Munoz-Crego, M. Joao Matos, S. Vazquez-Rodriguez, L. Santana, E. Uriarte, C. Fuentes-Edfuf, Y. Santos, A. Munoz-Crego, *Med. Chem.* **2012**, *8*, 1140.
[7] Y. Shi, C.-H. Zhou, *Bioorg. Med. Chem. Lett.* **2011**, *21*, 956.
[8] M. Manjunatha, V. H. Naik, A. D. Kulkarni, S. A. Patil, *J. Coord. Chem.* **2011**, *64*, 4264.
[9] M. Watzka, C. Geisen, C. G. Bevans, K. Sittinger, G. Spohn, S. Rost, E. Seifried, C. R. Müller, J. Oldenburg, *J. Thromb. Haemost.* **2011**, *9*, 109.
[10] S. Weigt, N. Huebler, R. Strecker, T. Braunbeck, T. H. Broschard, *Reprod. Toxicol.* **2012**, *33*, 133.
[11] A. A. H. Kadhum, A. A. Al-Amiery, A. Y. Musa, A. B. Mohamad, *Int. J. Mol. Sci.* **2011**, *12*, 5747.
[12] W. Qin, C. Liu, W. Jiang, Y. Xue, G. Wang, S. Liu, *BMC Microbiol.* **2019**, *19*, 50.
[13] M.-B. Nayeli, H.-R. Maribel, J.-F. Enrique, B.-P. Rafael, A.-F. Margarita, F.-M. Macrina, M.D. Ivan, G.C. Manasés *Nat. Prod. Res.* **2020**, *34*, 3244.
[14] C. Mu, M. Wu, Z. Li, *Chem. Biodiversity* **2018**, *16*, e1800559.
[15] N. Lv, M. Sun, C. Liu, J. Li, *Bioorg. Med. Chem. Lett.* **2017**, *27*, 4578.
[16] T. Nasr, S. Bondock, M. Youns, *Eur. J. Med. Chem.* **2014**, *76*, 539.
[17] N. S. Goud, M. S. Ghouse, J. Vishnu, J. Pranay, R. Alvala, V. Talla, I. A. Qureshi, M. Alvala, *Anticancer Agents Med. Chem.* **2019**, *19*, 557.
[18] T. K. Mohamed, R. Z. Batran, S. A. Elseginy, M. M. Ali, A. E. Mahmoud, *Bioorg. Chem.* **2019**, *85*, 253.
[19] L. J. Lombardo, F. Y. Lee, P. Chen, D. Norris, J. C. Barrish, K. Behnia, S. Castaneda, L. Cornelius, J. Das, A. M. Doweyko, C. Fairchild, J. T. Hunt, I. Inigo, K. Johnston, A. Kamath, D. Kan, H. Klei, P. Marathe, S. Pang, R. Peterson, S. Pitt, G. L. Schieven, R. J. Schmidt, J. Tokarski, M. L. Wen, J. Wityak, R. M. Borzilleri, *J. Med. Chem.* **2004**, *47*, 6658.
[20] Y. Chen, H.-R. Liu, H.-S. Liu, M. Cheng, P. Xia, K. Qian, P. C. Wu, C. Y. Lai, Y. Xia, Z. Y. Yang, S. L. Morris-Natschke, K. H. Lee, *Eur. J. Med. Chem.* **2012**, *49*, 74.
[21] X.-Q. Wu, C. Huang, Y.-M. Jia, B.-A. Song, J. Li, X.-H. Liu, *Eur. J. Med. Chem.* **2014**, *74*, 717.
[22] D. R. Vianna, L. Hamerski, F. Figueiró, A. Bernardi, L. C. Visentin, E. N. S. Pires, H. F. Teixeira, C. G. Salbego, V. L. Eifler-Lima, A. Battastini, G. L. von Poser, A. C. Pinto, *Eur. J. Med. Chem.* **2012**, *57*, 268.
[23] E. Bin Yang, Y. N. Zhao, K. Zhang, P. Mack, *Biochem. Biophys. Res. Commun.* **1999**, *260*, 682.
[24] N. S. Reddy, K. Gumireddy, M. R. Mallireddigari, S. C. Cosenza, P. Venkatapuram, S. C. Bell, E. P. Reddy, M. Reddy, *Bioorg. Med. Chem.* **2005**, *13*, 3141.
[25] K. N. Venugopala, V. Rashmi, B. Odhav, *BioMed Res. Int.* **2013**, *2013*, 1.
[26] K. M. Amin, A. A. M. Eissa, S. M. Abou-Seri, F. M. Awadallah, G. S. Hassan, *Eur. J. Med. Chem.* **2013**, *60*, 187.
[27] B. Kahveci, F. Yılmaz, E. Menteşe, S. Ülker, *Arch. Pharm. (Weinheim)* **2017**, *350*, 1600369.
[28] R. Z. Batran, D. H. Dawood, S. A. El-Seginy, M. M. Ali, T. J. Maher, K. S. Gugnani, A. N. Rondon-Ortiz, *Arch. Pharm. (Weinheim)* **2017**, *350*, 1700064.
[29] K. M. Amin, A. M. Taha, R. F. George, N. M. Mohamed, F. F. Elsenduny, *Arch. Pharm. (Weinheim)* **2018**, *351*, 1700199.
[30] E. Menteşe, A. Güner, E. Polatlı, M. Emirik, H. Bektaş, B. Kahveci, *Arch. Pharm. (Weinheim)* **2020**, *354*, 2000284.
[31] M. M. Ghorab, M. S. Alsaid, Y. M. Nissan, *Life Sci. J.* **2013**, *10*, 2170.
[32] M. M. Ghorab, M. S. Alsaid, M. S. A. El-Gaby, M. M. Elaasser, Y. M. Nissan, *Chem. Cent. J.* **2017**, *11*, 32.
[33] M. M. Ghorab, M. S. Alsaid, M. S. Al-Dosary, Y. M. Nissan, S. M. Attia, *Chem. Cent. J.* **2016**, *10*, 19.
[34] M. M. Ghorab, M. S. Alsaid, Y. M. Nissan, *Acta Pol. Pharm.* **2014**, *71*, 603.
[35] M. M. Ghorab, M. S. Al-Said, Y. M. Nissan, *Arzneimittelforschung* **2012**, *62*, 497.
[36] M. M. Ghorab, M. S. Alsaid, M. S. Al-Dosari, Y. M. Nissan, A. A. Al -Mishari, *Chem. Cent. J.* **2016**, *10*, 18.
[37] M. M. Ghorab, F. A. Ragab, H. I. Heiba, H. M. Agha, Y. M. Nissan, *Arch. Pharm. Res.* **2012**, *35*, 59.
[38] F. W. Canter, F. H. Curd, A. Robertson, *J. Chem. Soc.* **1931**, *0*, 1255.
[39] A. Kathuria, N. Priya, K. Chand, P. Singh, A. Gupta, S. Jalal, S. Gupta, H. G. Raj, S. K. Sharma, *Bioorg. Med. Chem.* **2012**, *20*, 1624.
[40] E.-M. Kwon, C.-G. Kim, A.-R. Goh, J.-S. Park, J.-G. Jun, *Bull. Korean Chem. Soc.* **2012**, *33*, 1939.
[41] N. Kumar, *World Res. J. Biochem.* **2012**, *1*, 2279.
[42] E. Bombardelli, P. Valenti, *US6767916B2* **2004**.
[43] K. V. Sashidhara, A. Kumar, M. Kumar, J. Sarkar, S. Sinha, *WO/2012/017454* **2014**.
[44] M. V. Berridge, P. M. Herst, A. S. Tan, *Biotechnol. Annu. Rev.* **2005**, *11*, 127.
[45] T. Mosmann, *J. Immunol. Methods* **1983**, *65*, 55.
[46] Enzyme-Linked Immunosorbent Assay Kit, www.arp1.com (accessed: July 2017).
[47] N. E. Hynes, H. A. Lane, *Nat. Rev. Cancer* **2005**, *5*, 341.
[48] G. M. Morris, R. Huey, W. Lindstrom, M. F. Sanner, R. K. Belew, D. S. Goodsell, A. J. Olson, *J. Comput. Chem.* **2010**, *30*, 2785.
[49] E. F. Pettersen, T. D. Goddard, C. C. Huang, G. S. Couch, D. M. Greenblatt, E. C. Meng, T. E. Ferrin, *J. Comput. Chem.* **2004**, *25*, 1605.
[50] N. M. O'Boyle, M. Banck, C. A. James, C. Morley, T. Vandermeersch, G. R. Hutchison, *J. Cheminf.* **2011**, *3*, 33.
[51] A. Daina, O. Michielin, V. Zoete, *Sci. Rep.* **2017**, *7*, 1.
[52] A. Daina, V. Zoete, *ChemMedChem* **2016**, *11*, 1117.
[53] C. A. Lipinski, *Curr. Drug Discov.* **2001**, *1*, 17.

SUPPORTING INFORMATION

Additional Supporting Information may be found online in the supporting information tab for this article.

How to cite this article: F. A. Ragab, A. A. M. Eissa, S. H. Fahim, M. A. Salem, M. A. Gamal, Y. M. Nissan. Synthesis and biological evaluation of new coumarinderivatives as cytotoxic agents, *Arch. Pharm.* **2021**, 354, e2100029. https://doi.org/10.1002/ardp.202100029